



# Selective load control of lumbar muscles in robot-assisted isometric lumbar stabilization exercise

Joowan Kim<sup>1,2</sup> · Wonje Choi<sup>3</sup> · Jaeheung Park<sup>1,4</sup> 

Received: 20 September 2023 / Accepted: 20 February 2024  
© The Author(s) 2024

## Abstract

Lumbar stabilization exercises are commonly employed in the rehabilitation of patients with low back pain. However, many patients discontinue these exercises, generally calisthenics using various postures or tools, due to the difficulty of providing an appropriate exercise load intensity. This challenge results in an inability to apply the desired strength to the target lumbar muscles and sometimes leads to an excessive load on unintended areas during calisthenics. Consequently, a method that enables patients to exercise continuously and progressively recover is required, specifically one that can target the lumbar muscles with a desired load. To address this issue, we propose a rehabilitation assistive device that quantitatively controls the lumbar spine load. In isometric lumbar stabilization exercises, our method involves precise compensation for gravity. The device, equipped with a series elastic actuator, is positioned beneath the patient in a lying posture. It applies an assistive force in the direction opposite to gravity, enabling precise control of the load on the lumbar region and reducing the vertical load on the spine. To validate the effectiveness of our proposed method, we conducted experiments with 20 healthy subjects across three exercises and analyzed the electromyography signal using nonparametric statistical methods. Our objective was to determine whether the load on the target lumbar muscles could be precisely and gradually controlled. The statistical results indicate that exercises performed using the proposed device produce statistically significant load changes in the target lumbar muscles.

**Keywords** Low back pain · Lumbar stabilization exercise · Assistive device · Series elastic actuator

## 1 Introduction

Low back pain (LBP) is a prevalent and severe health issue worldwide. The lifetime prevalence of LBP in developed

---

Joowan Kim and Wonje Choi have contributed equally to this work.

✉ Jaeheung Park  
park73@snu.ac.kr

Joowan Kim  
joowan@snu.ac.kr

Wonje Choi  
wj82.choi@samsung.com

<sup>1</sup> Graduate School of Convergence Science and Technology, Seoul National University, Seoul 08826, Republic of Korea

<sup>2</sup> Department of Rehabilitation Medicine, Seoul National University Hospital, Seoul 03080, Republic of Korea

<sup>3</sup> Samsung Advanced Institute of Technology, Suwon 16678, Republic of Korea

<sup>4</sup> Advanced Institute of Convergence Technology, Suwon 16229, Republic of Korea

countries is estimated to be 60–70% [1] and is notably high in middle-aged and older groups [2]. Causes of LBP can include trauma, infection, tumor, osteoporosis, and herniated disks. Prolonged LBP can lead to a deterioration in patient health. Research indicates that 30–40% of LBP patients progress to a subacute state (>6 weeks), and 10–20% evolve into a chronic condition (>12 weeks) [3]. Additionally, chronic patients are at risk of developing further complications and experiencing economic difficulties, such as job loss and high medical expenses [4].

Exercise therapy is an effective approach for improving the condition of LBP patients. These therapies are diverse, ranging from general physical fitness or aerobic exercises for muscle strengthening to various flexibility and stretching exercises [5]. Several medical guidelines, supported by substantial clinical evidence, recommend specific rehabilitation exercises for alleviating pain and enhancing daily activities in LBP patients [6, 7]. Lumbar stabilization exercise (LSE) is particularly recommended, based on Panjabi's spine stability theory, which provides a mechanical understanding of

LBP [8]. Evidence supports LSE's effectiveness in improving lumbar stability [9, 10], providing pain relief, and enhancing function within a short therapeutic time [11]. Additionally, LSE can effectively prevent LBP recurrence [12].

However, like other exercise methods for LBP, LSE cannot be deemed a universally reliable method. A significant factor contributing to this limitation is the substantial body load that patients must endure while performing the exercise [13]. Exercise loads, critical in nature, are categorized into the load on the lumbar muscles and the load on other body parts. The problem is that the calisthenics used as lumbar stabilization exercises require a significant load on the muscles that fall into both of those two categories. Also, traditional LSE methods often overlook the need for quantitative and precise load adjustment of the lumbar muscles; consequently, facilitating progressive recovery of lumbar stability through gradual load increase remains challenging. Moreover, the excessive load on other body parts can render LSE challenging for many patients to perform comfortably and accurately, thus diminishing its potential benefits.

This study introduces a device engineered for precise and quantitative control of muscle load in LSE. We evaluated the device's efficacy through exercise experiments and statistical analysis. By controlling the force of a series elastic actuator (SEA), the proposed device facilitates precise control of muscle load on the lumbar spine, obviating the need for patients to alter their posture. The findings demonstrate that the proposed device can precisely control the load on the targeted lumbar muscles.

In a previous study, we proposed a hardware device for lumbar stabilization exercise (LSE) and reported pilot results indicating that exercise using the device yielded muscle activation patterns similar to those of calisthenics. It was also observed that muscle load could be adjusted through the device [14]. However, we noted that exercise using the device for specific exercises demonstrated different muscle patterns compared to calisthenics. To address this issue, an improved device, based on feedback from preclinical trials, was proposed [15].

This paper addresses another aspect, specifically, the feasibility of fine load control on target muscles through experiments. In this paper, precise load control refers to the regulation of the magnitude of the load applied to the lumbar muscles of the subjects. Even with precise control of the output force of the SEA, it is not guaranteed that the actual load on the target lumbar muscles will be precisely regulated for each exercise performed by the subjects. This is due to the complexity of the lumbar muscles and the fact that each subject engages muscles differently, even when performing the same exercise. Furthermore, without precise control of the load, it is impossible to ensure that the patient receives an appropriate exercise load. Therefore, precise control of

the lumbar muscle load is one of the most crucial aspects to verify in the proposed device.

For this purpose, experiments were conducted using the existing IRB-approved device [14]. Additionally, this study incorporated an enhanced controller designed to reduce impedance force and minimize force error caused by human movement disturbances. In the LSE utilizing the device, a systematic dynamics analysis was carried out to anticipate changes in muscle load. An experiment involving 20 healthy subjects was conducted to verify the exercise effect. Muscle activity was measured using surface electromyography (sEMG) sensors during exercise with the device. Given the increased number of subjects compared to the previous study, nonparametric statistical analysis was employed. The results demonstrate that the proposed device enables precise load control on the lumbar muscles. Additionally, the experimental results show statistically significant changes even in the smallest differences in muscle activation when compared to previous studies.

Furthermore, an in-house survey was conducted to assess participants' experiences during the exercise [16]. The survey results confirmed that the proposed device was effective in reducing muscle load not only in the lumbar region but also in other areas. Additionally, it induced changes in motion perception among the subjects.

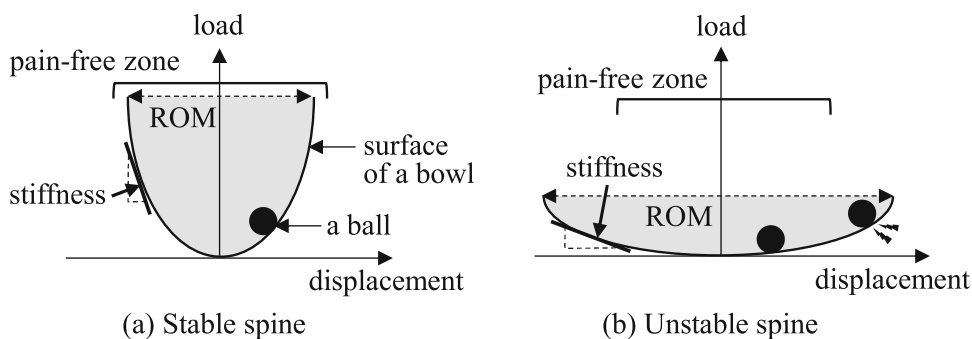
## 2 Concept and proposed method for the lumbar stabilization exercise

### 2.1 Spine stability

Panjabi's [8] theory of spinal stability conceptualizes spinal stability by subdividing the spinal system into three subsystems, thereby elucidating the physical mechanisms of LBP and spinal instability. A significant correlation between spinal stability and LBP is also presented in related studies [17, 18].

The concept of spinal stability can be understood through the ball-in-a-bowl analogy, as illustrated in Fig. 1 [19]. In this analogy, the ball represents spinal displacement under the specific load; the bowl surface depicts load characteristics corresponding to the displacement; the nonlinear slope of the bowl surface indicates spinal stiffness; and the bowl's width represents the spine's range of motion (ROM). For a stable spine, as shown in Fig. 1a, high spinal stiffness is necessary, and ROM should be within the pain-free zone. Pain occurs when a large load is applied to the spine, displacing it outside the ROM. Conversely, in an unstable spine, as depicted in Fig. 1b, stiffness is lower, and ROM is wider than in a stable spine. Therefore, even with a relatively small load, the spine can move abnormally out of the pain-free motion zone, causing pain to tissues or nerves.

**Fig. 1** Ball-in-a-bowl analogy for spine stability



**2.2 Load issues in lumbar stabilization exercises**

Lumbar stabilization exercise (LSE) consists of isometric exercises that train specific lumbar muscles by requiring patients to maintain a certain posture for a defined period. The objective is to enhance the strength, endurance, and control of the spinal muscles, thereby improving lumbar stability. Gradual increase in the LSE load can progressively enhance spinal stability, enabling patients to support a larger load with minimal displacement, as illustrated in Fig. 2a.

However, the challenge with LSE for LBP patients lies not in the posture, but in the load each muscle must endure during exercise. In LSE, a posture is maintained by supporting the whole or part of the body weight with the strength of the upper limbs, lower limbs, and lower back, as depicted in Fig. 2b. Consequently, various lumbar muscles are subjected to different magnitudes of force load. Let  $l_{req_i}$  ( $i = 1, 2, \dots, n$ ) represent the load required for each lumbar muscle.  $n$  represents the number of lumbar muscles contributing to lumbar stabilization exercises. The vector  $L_{req}$ , representing the load required for the muscles when performing LSE, can be expressed as follows:

$$\vec{L}_{req} = [l_{req_1}, l_{req_2}, \dots, l_{req_n}] \tag{1}$$

Additionally, let  $l_{cap_i}$  represent the load that each muscle can withstand during the exercise without pain, at a moderate level. Consequently, the load capacity of the muscles,  $L_{cap}$ , which a person can endure without experiencing pain, can be

expressed as the following vector:

$$\vec{L}_{cap} = [l_{cap_1}, l_{cap_2}, \dots, l_{cap_n}] \tag{2}$$

For moderate level exercising, each muscle can have a capacity load larger than the load requirement of LSE for all muscles in that patient, expressed as follows:

$$l_{cap_i} > l_{req_i} \text{ (for every muscle } i) \tag{3}$$

Nevertheless, patients with LBP are more likely to have weakened lumbar muscles. In addition, exercise may be risky because  $L_{req}$  is increased by the patient’s weight. Moreover, the strengths of the upper and lower limbs also decide whether exercising can be unsafe for the patients. Therefore, it is highly unlikely that the condition (3) is satisfied. Hence, a cautious approach is suggested when training patients with chronic LBP. As an example of this issue, previous research has stated that this problem can also arise when performing McGill’s Big 3 exercises, which are frequently used LSE in clinical settings [20].

Therefore, providing a personalized and gradual exercise load can increase the completion rate of LSE among patients. Previous studies on LSE have modified the posture, incorporated weighted objects [21], and utilized tools such as a Swiss ball to adjust posture control difficulties [22]. Among these methods, altering the exercise posture is most commonly employed to reduce the load. This alteration is akin to changing the direction of the vector  $L_{req}$ . However, due to the complex interplay of various muscles, accurately predicting changes in  $L_{req}$  when altering posture is challenging. This is

**Fig. 2** Loads in a lumbar stabilization exercise

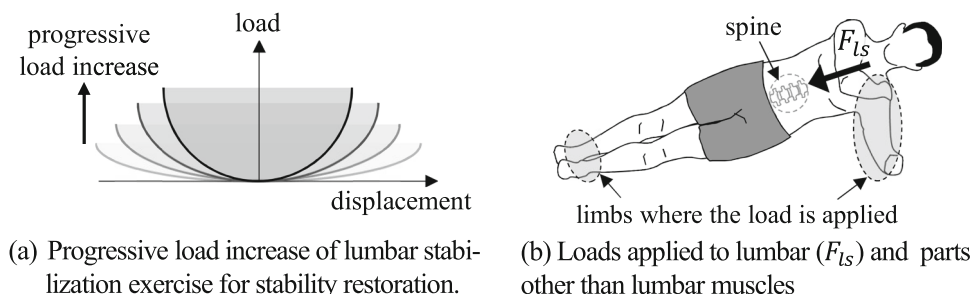
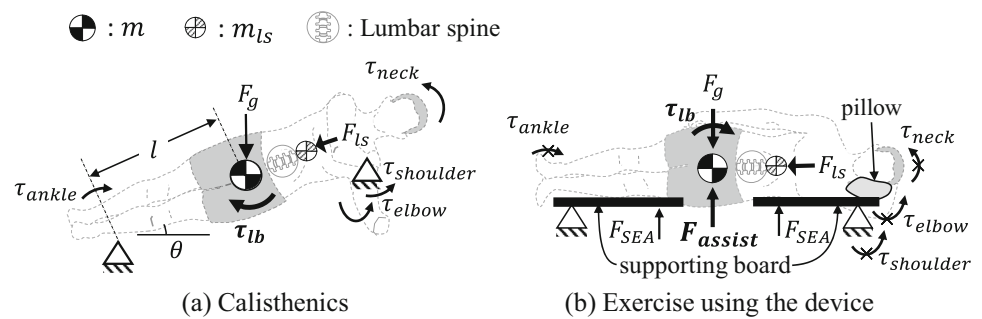


**Fig. 3** Calisthenics and exercise using the proposed device



especially true for LBP patients, as individual conditions can vary significantly. Additionally, the absence of a quantitative exercise standard complicates the numerical and precise control of the load on the patient. Conventional methods can provide several load levels, offering statistically significant differences of 5-15% based on normalized muscle activity. However, there are numerous instances where no significant differences in exercise effectiveness are observed, even with load changes.

Building on the aforementioned analysis, our objective is to fine-tune the magnitude of the vector  $L_{req}$  while minimizing changes in its direction. To this end, we have developed a rehabilitation exercise device that can fine-tune the load on the lumbar muscles without changing the exercise posture.

### 2.3 Proposed method for adjusting lumbar load

There are various methods to adjust the load on the lumbar muscles without altering the posture. To illustrate these methods, we simplify the Big 3 exercise's side-bridge (SB) posture as an example, treating it as a rotational joint with one degree of freedom (DOF). The upper and lower body can be represented as two links connected by a lumbar joint. The body parts on the ground are represented as supporting points. The supporting points act as rotary joints and withstand the body weight to balance. The body segmental mass in relation to the lumbar can be expressed as a point mass  $m$ . In the general LSEs, the human system can be modeled with one or two supporting points and point masses.

Then, the lumbar torque is determined by the gravity force  $F_g (= mg)$  and length  $l$  between the supporting point and point mass. In addition, the torque exerted on other body parts, such as the ankle, shoulder, elbow, and neck, also influences lumbar torque, as shown in Fig. 3a.

Thus, the lumbar torque  $\tau_{lb}$  can be expressed as follows:

$$\tau_{lb} = F_g \cdot l \cdot \cos \theta \quad (4)$$

where  $F_g$  is the gravity force,  $l$  is the lengths of the upper and lower body, and  $\theta$  is the angle between the body and ground.

From Eq. (4), we adopted the adjustment of  $F_g$  among  $F_g$ ,  $l$ , and  $\theta$  as a variable to control the lumbar load. The method

of changing the load by changing  $l$  has been widely adopted in sling exercises. However, due to the body's nonlinear shape, a change in  $l$  was anticipated to result in a nonlinear change in the lumbar load.

Additionally, altering the point of support to adjust  $l$  can substantially modify the muscle load pattern throughout the subject's body. For example, as demonstrated in the exercise depicted in Fig. 3a, the set of lower body and lumbar muscles activated while supporting the calf differs from those engaged during thigh support. Consequently, narrowing the range of  $l$  to circumvent this variability simultaneously diminishes the scope of load control.

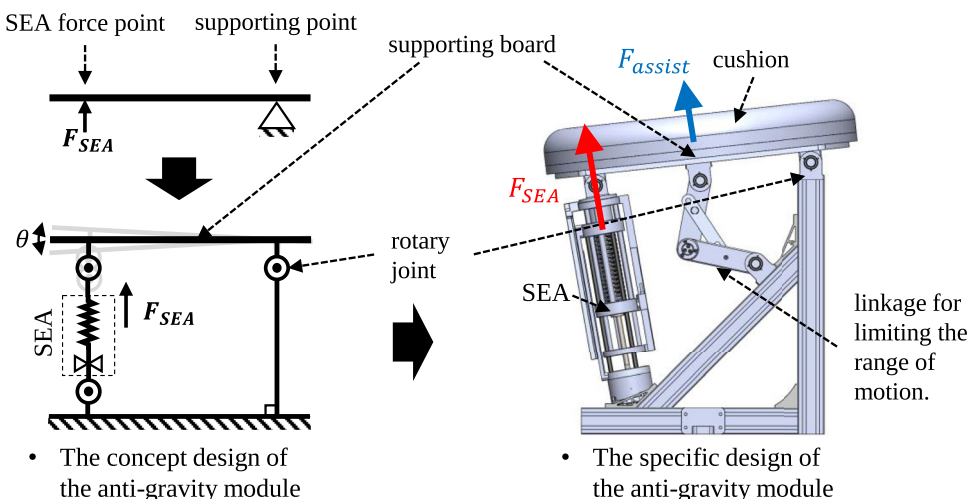
The commercial product Centarus adjusts the  $\theta$  value [23]. However, we overlook this method because the vertical load  $F_{ls}$  applied to the lumbar changes according to changes in  $\theta$ , as shown in Fig. 3a. This is because when the body is placed in an upright position to reduce the load, the load on the erector spinae muscle increases, and the vector of the lumbar load changes unexpectedly.

The method proposed in this study is to precisely control the gravitational force  $F_g$  through gravity compensation. Through this method, the load required on the lumbar can be adjusted to that which the patient can withstand. In addition, there is no need to change the posture. The most critical aspect to note is that, as both the support point and the center of gravity remain constant, only the variations in load caused by gravitational force  $F_g$  impact the lumbar muscles. Moreover, the absence of a need for posture adjustment in response to load alteration ensures that load changes do not significantly change muscle usage in other body parts, including the lumbar region. Lastly, our proposed approach allows exercises to be performed in a supine position, minimizing the vertical load  $F_{ls}$  on the spine.

The load adjustment process is as follows: The proposed device applies an assistive force  $F_{assist}$  in the direction opposite to the gravitational force  $F_g (= m \cdot g)$ . Consequently, the resulting torque on the lumbar spine,  $\tau_{lb}$ , as illustrated in Fig. 3b, can be expressed as follows:

$$\begin{aligned} \tau_{lb} &= (F_g - F_{assist}) \cdot l \cdot \cos \theta, \\ F_{assist} &= \alpha \cdot F_g \end{aligned} \quad (5)$$

**Fig. 4** Design of the anti-gravity module



where  $\alpha$  is the assistance ratio.  $\alpha = 1$  indicates that zero load is applied to the lumbar and the power is provided by human muscles without gravity compensation.

As angle  $\theta$  is 0 due to the lying position, combining the two equations in Eq. (5), we get the quantitatively adjusted lumbar torque  $\tau_{lb}$  as follows:

$$\tau_{lb} = (1 - \alpha) \cdot F_g \cdot l \tag{6}$$

If there is a linear relationship between the muscle and  $\alpha$ , the load on each muscle needed for exercise can be expressed as follows:

$$\vec{L}_{req} = (1 - \alpha) \cdot [l_{req1}, l_{req2}, \dots, l_{reqn}] \tag{7}$$

Thus, the load element and exercise posture determine the magnitude and direction of  $L_{req}$ , respectively. In practice, the relationship between  $\alpha$  and the whole body muscles will be nonlinear due to the complex relationship between the muscles. Therefore, monotonically decreasing the load on the whole body muscles with increasing  $\alpha$  is challenging. Despite the nonlinearity, an increase in  $\alpha$  is expected to decrease the load on the target lumbar muscles monotonically when exercising. Therefore,  $\alpha$  should control the magnitude of each lumbar muscle. This study verifies the aforementioned hypothesis through statistical analysis of the experimental results.

### 2.4 Device design for implementing the proposed method

The device was designed to implement the method proposed in Fig. 3b. The proposed method provides supporting points to support a part of the body. A series elastic actuator (SEA) implements the gravity compensation  $F_{assist}$ . Additionally, a supporting board between the assist force and supporting

points acts as a link and restricts the movement of other joints. The anti-gravity module comprises a supporting point, assist force point, and supporting plate, as shown in Fig. 4.

In the specific device, the supporting point and force source are implemented as a rotary joint and an SEA, respectively. The supporting board is made of a mattress for safety and soft contact with the subject. The device uses two modules, as shown in Fig. 5a, to perform LSE. Both modules can be rotated and translated to adjust the load on various lumbar muscles due to different exercise postures. In addition, the modules can be arranged according to human body sizes. Finally, as shown in Fig. 5b, the subject performs LSE while lying on the device. Detailed specifications of the device are introduced in [14].

### 2.5 Dynamics analysis of exercise using the proposed device

Among the various proposed lumbar stabilization exercises, the Big 3 exercises are a prominent and recommended method for LBP patients. The Big 3 exercises proposed by McGill can train most of the lumbar muscles with only three postures and is used to demonstrate the working of the proposed device [24, 25]. The Big 3 exercises consists of three postures: curl-up (CU), side-bridge (SB), and bird-dog (BD) posture. The Big 3 exercises were chosen for our study as they are the most commonly used and clinically proved to be effective methods in the medical field.

Detailed muscle activation results for these exercises are provided in [26]. The exercise trains the following lumbar muscles: rectus abdominis (RA), external oblique (EO), internal oblique (IO), thoracic erector spinae (TE), and lumbar erector spinae (LE), as shown in Fig. 6a.

These muscles contribute differently to the torque and movement of the lumbar, as shown in Fig. 6b. For example, RA, EO, and IO muscles are used for trunk flexion, EO,



Fig. 5 Specific design of the device

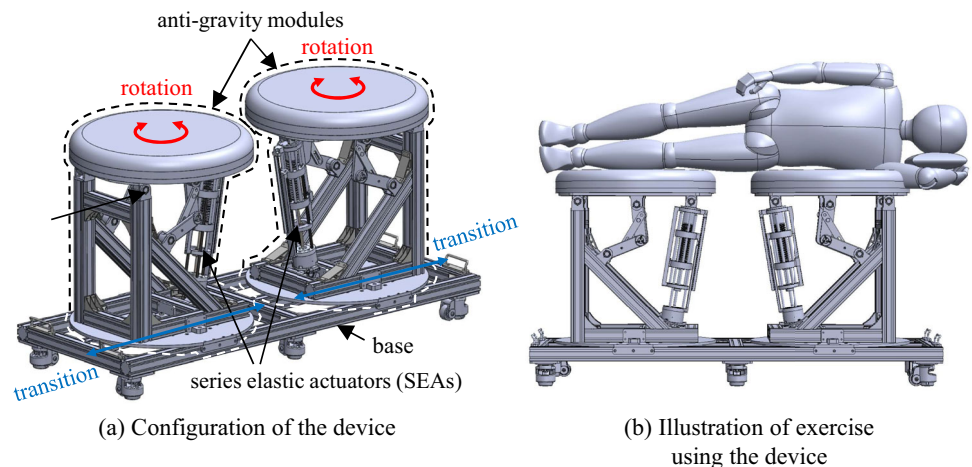
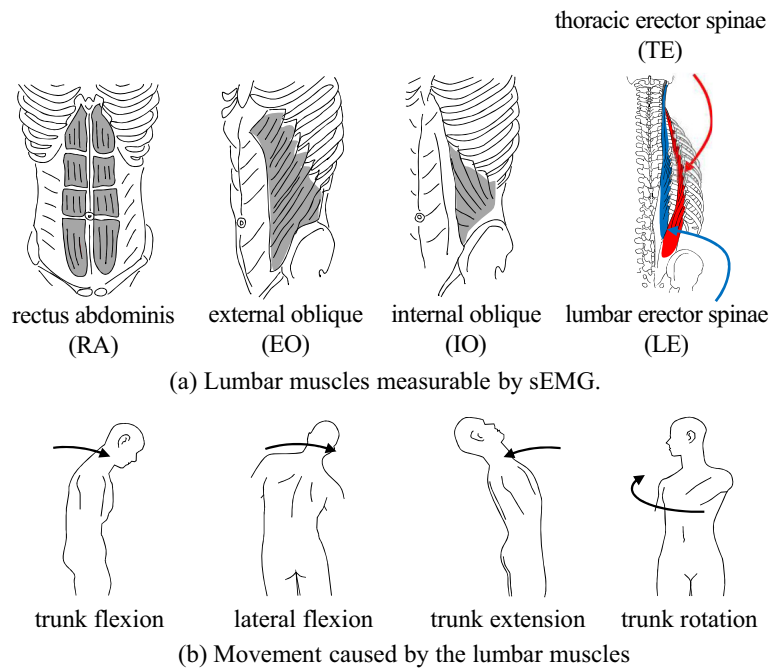


Fig. 6 Lumbar muscles and movements associated with the lumbar spine



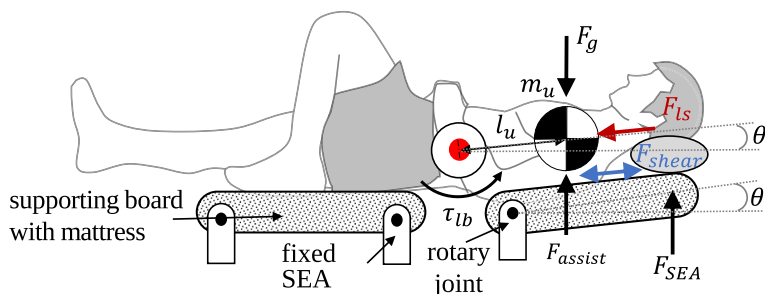
IO, and LE muscles for lateral flexion, TE and LE muscles for trunk extension, and EO and IO muscles for trunk rotation.

**Explanation of the simplified modeling approach:** In the proposed device, the interaction forces between the human and the device during exercise are complex. Figure 7 presents a simplified model of the curl-up exercise, the easiest to model among the three exercises. In reality, the assistive force  $F_{assist}$  is generated by the torque from the device's rotation in contact with the subject. Additionally, there are forces acting along the spine direction,  $F_{ls}$ , and shear forces between the subject and the device,  $F_{shear}$ . Therefore, the torque exerted on the subject can be expressed as follows, assuming that  $F_g$ ,  $F_{assist}$ , and  $F_{SEA}$  are all vertically oriented:

$$\tau_{lb} = F_g \cdot l_u + F_{ls} \cdot l_u \cdot \sin \theta + F_{shear} \cdot l_u \cdot \sin \theta - F_{assist} \cdot l_u \tag{8}$$

$F_{assist}$  represents the virtual force exerted by  $F_{SEA}$  on the upper body's center of mass,  $m_u$ , in the vertical direction through the device. Since the two forces have different moment arms,  $F_{assist}$  can be described as follows, considering the characteristics of the device (assuming that the angle between the device and the ground is the same as the angle between the subject and the ground).

**Fig. 7** Explanation of a simplified model through dynamics analysis



$$F_{assist} = \frac{l_{SEA}}{l_{assist}} \cdot F_{SEA} \tag{9}$$

However, in Eq. (8),  $F_{ls}$  and  $F_{shear}$  can be considered negligible in terms of their vertical direction components during the lying-down exercise. Therefore, they can be simplified as follows:

$$\tau_{lb} = (F_g - F_{assist}) \cdot l_u \tag{10}$$

We intend to provide a simplified explanation by focusing on the utilization of  $F_g$  and  $F_{assist}$  in the analysis of each exercise posture. The main emphasis of this paper is to investigate whether the SEA can precisely adjust the muscle load on the lumbar spine. Hence, we employ a simplified modeling approach to facilitate comprehension of the forces exerted by the device during various exercises.

The first design objective of the exercise protocol was to adjust the load on the training muscles to render the training muscles when using the device similar to when performing calisthenics. The second objective was to reduce the load other than that on the lumbar. Therefore, the posture of the calisthenics was kept the same as possible, while that using the proposed device was modified to meet the design objectives. The exercise protocols using the device for the Big 3 exercises are described as follows:

**Curl-up (CU):** CU is a single-degree-of-freedom exercise that applies torque of trunk flexion, and Fig. 8a, b shows the calisthenics and the exercise using the device, respectively. In CU using the device,  $F_{assist}$  alleviates the lumbar torque  $\tau_{lb}$  on the experiment subject as follows:

$$\begin{aligned} \tau_{lb} &= (F_g - F_{assist}) \cdot l_u = (1 - \alpha) \cdot F_g \cdot l_u \\ &= (1 - \alpha) \cdot m_u \cdot g \cdot l_u \end{aligned} \tag{11}$$

where  $m_u$  is the mass of the upper body, and  $l$  is the length between the rotary joint of the module and point  $m_u$ . The angle between the upper body and ground is ignored here.

The exercise protocol for using the device is as follows: To apply a force  $F_{assist}$ , only one end of the module under the upper body is fixed, while the module under the lower body is fixed at both ends. The SEA in the module beneath

the upper body is positioned close to the head. A pillow is used to mitigate the load on the neck muscles. The umbilicus is centrally placed between the two modules, approximately 5 cm away from each module joint. In calisthenics, the lumbar joint is close to the chest, as depicted in Fig. 8a, but it is positioned nearer to the lumbar region when using the device. This positioning is due to the anticipated small adjustable torque range, attributed to the low  $m_u$  and short  $l$ . The RA, EO, and IO muscles, which facilitate trunk flexion, are primarily activated. Among these muscles, the proportion of RA activation is expected to decrease, owing to the changes in the rotation axis.

**Side-bridge (SB):** The SB is an exercise with a single degree of freedom that applies torque for lateral flexion. Unlike the simplified SB model depicted in Fig 3b, the actual proposed device employs two Series Elastic Actuators (SEAs) to apply  $F_{SEA,l}$  and  $F_{SEA,u}$  to the upper and lower body segments, respectively. This results in the generation of  $F_{assist,l}$  and  $F_{assist,u}$ . The  $F_{assist}$  in Fig 3b represents the combined resultant force of  $F_{assist,l}$  and  $F_{assist,u}$ .

The SB exercises in calisthenics and those using the device are depicted in Fig. 8c, d, respectively. Compared to the model in Fig. 8d, the model in Fig. 8c differs from the previous model in Fig. 3, with the point mass being divided between the upper and lower body segments.

Although the lumbar joint can be considered a 1-DOF system, unlike in the curl-up exercise, two SEAs apply the assistive force in a lateral direction. When the device assists the subject, the lumbar torque  $\tau_{lb}$  is determined as follows:

$$\begin{aligned} \tau_{lb} &= (1 - \alpha) \cdot (F_{g,u} \cdot l_u + F_{g,l} \cdot l_l) \\ &= (1 - \alpha) \cdot (m_u \cdot l_u + m_l \cdot l_l) \cdot g \end{aligned} \tag{12}$$

where  $F_{g,u}$  and  $F_{g,l}$  are the gravity forces applied to the upper and lower body, respectively; and  $m_u$  and  $m_l$  are point masses of the upper and lower body concentrated on the locations at each SEA, respectively.

The detailed exercise protocol is as follows: The subject's shoulder joint is positioned above the module joint for the upper body, and the ankle joint is placed 5 cm outside the module joint for the lower body. In this protocol, unlike in the calisthenics of the side-bridge (SB), the limbs are rested

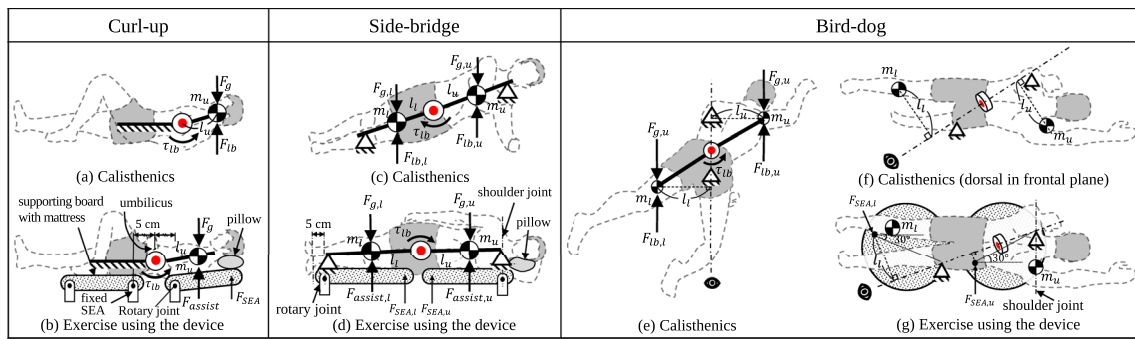


**Fig. 8** Big 3 exercise postures comparison in calisthenics (a), (c), (e), and (f) and when exercise using the device (b), (d), and (g)

during the exercise. Consequently, patients with diseases or lack of strength in the upper or lower limbs can perform this exercise comfortably. The most actively engaged muscles in the designed protocol are likely the EO, IO, and LE muscles, as these are responsible for lateral flexion motion similar to calisthenics.

**Bird-dog (BD):** The BD is a multi-degree-of-freedom exercise that simultaneously applies torque for trunk extension and trunk rotation. The postures of lifting the right hand and left knee in the bird-dog exercise are depicted in Fig. 8e–g. As illustrated in Fig. 8e, the lumbar joint, which is a 1-DOF system, aligns with the right shoulder and left thigh. The required torque compensates for the forces  $F_{g,u}$  and  $F_{g,l}$ , which are due to the point masses  $m_u$  and  $m_l$  on the right upper and left lower body, respectively. With the assistive force, the lumbar torque  $\tau_{lb}$  can be expressed as follows:

$$\begin{aligned}\tau_{lb} &= (1 - \alpha) \cdot (F_{g,u} \cdot l_u + F_{g,l} \cdot l_l) \\ &= (1 - \alpha) \cdot (m_u \cdot l_u + m_l \cdot l_l) \cdot g\end{aligned}\quad (13)$$

Here,  $l_u$  and  $l_l$  represent the lengths of the moment arms for the upper and lower body, respectively. Taking into account the expected limb masses in the calisthenics BD, the modules are positioned as shown in Fig. 8g. The dotted circle represents the supporting board, the triangle indicates the supporting point, and the circle with a cross symbolizes the point mass position, which is also the assist force point of the Series Elastic Actuator (SEA).

However, in the BD exercise, the point of force application by the SEA differs from the center of mass of the upper and lower body segments, with a particularly noticeable difference in the upper body segment. This discrepancy is attributed to the abdomen drooping under the influence of gravity between the two supporting points. Therefore, we modified the exercise protocol for device use. Consequently, the position of the SEA in the upper body module was relocated closer to the lumbar region to decrease the load adjustment range by reducing  $l_u$ .

The final protocol, as illustrated in Fig. 8g, involves rotating each module by 30 degrees. The left shoulder is positioned over the supporting point of the upper body module, and the center of the right thigh is placed above the supporting joint of the lower body module. The protocol for the exercise that involves lifting the left arm and right leg in the BD exercise is symmetrical to the aforementioned arrangement.

The new design protocol is expected to reduce the load adjustment range of the right TE, which is directly related to the trunk extension because of decreasing  $l_u$ . The right LE supports the right knee on the ground and controls the posture in the calisthenics in Fig. 8e. However, it was expected to be activated less in the device in Fig. 8g because the right thigh is almost fixed on the mattress. Additionally, the RA, EO, and IO muscles responsible for the trunk flexion were expected to maintain posture against the dropping abdomen.

## 3 Experimental methods

### 3.1 Controller for reducing impedance of SEA

In previous studies utilizing SEA, the controllers employed did not take into account the impedance caused by the movement of the subjects during exercise due to their different purposes. However, in the experiments conducted for this paper, an improved controller was applied to the SEA used, specifically designed to reduce force errors resulting from impedance.

In the proposed device, the SEA should regulate constant force with small errors to achieve the desired purpose when using the device. The displacement  $x_l$  dominantly influences the output force  $F_l$  of the SEA and its error due to disturbances from human movement. This relationship can be described using the concept of impedance  $Z$ , which is the transfer function between  $F_l$  and  $x_l$ . The proposed controller is designed to minimize the impact of  $x_l$  on  $F_l$  by reducing the impedance  $Z$  of the controlled SEA.



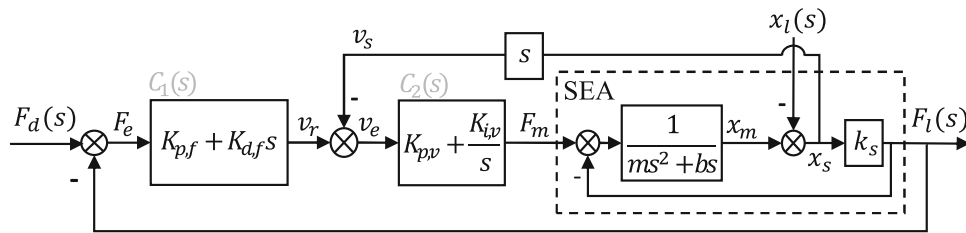


**Fig. 9** Force controller of SEA: The cascaded PD–PI controller with spring deformation rate feedback in the inner loop (CSRf). ( $F_d$ : desired force,  $C_1$ : primary controller with force feedback,  $v_r$ : reference velocity,  $v_m$ : motor velocity,  $v_s$ : velocity of spring deformation,  $v_l$ : velocity

of external motion,  $C_2$ : secondary controller with velocity feedback,  $F_m$ : motor force,  $x_l$ : external motion,  $x_s$ : deformation of spring in SEA,  $F_l$ : output force by SEA)

A cascade controller with motor velocity feedback (CMVF), which is commonly utilized in SEAs, was used as the SEA controller in our first prototype [14]. This controller offers robustness against friction and passivity [27]; however, the high impedance limits its application. To achieve lower impedance, this study employed a cascade controller with spring deformation rate feedback (CSRf). In CSRf, a PD controller is adopted as the primary controller  $C_1(s)$ , and the inner loop feedback is altered to the spring deformation rate  $v_s$ . The resulting controller is effectively equivalent to a single loop PID controller with a low-pass filter, as illustrated in Fig. 9. CSRf exhibits lower impedance  $Z$  compared to CMVF, which is why it was chosen over CMVF in this study. The impedance  $Z_{CMVF}$  of CMVF is calculated as follows:

$$Z_{CMVF}(s) = \frac{ms^4 + (b + K_{p,v})s^3 + K_{i,v}s^2}{\frac{m}{k_s}s^4 + \frac{D_1}{k_s}s^3 + D_2s^2 + K_{p,f}K_{i,v}s + K_{i,f}K_{i,v}} \quad (14)$$

$Z_{CSRf}$  of CSRf is calculated as follows:

$$Z_{CSRf}(s) = \frac{ms^4 + bs^3}{\frac{m}{k_s}s^4 + \frac{D'_1}{k_s}s^3 + D'_2s^2 + K_{p,f}K_{i,v}s + K_{i,f}K_{i,v}} \quad (15)$$

The notations in the aforementioned equations are consistent with those described in Fig. 9 and Table 1. The coefficients  $D_1$ ,  $D'_1$ ,  $D_2$ , and  $D'_2$  are represented as the follows.

$$D_1 = b + K_{p,v}, \quad D'_1 = D_1 + K_{p,v} \cdot K_{d,f} \cdot k_s \quad (16a)$$

$$D_2 = K_{p,f}K_{p,v} + \frac{K_{i,v}}{k_s} + 1, \quad D'_2 = D_2 + K_{i,v} \cdot K_{d,f} \quad (16b)$$

For the same parameter values, the numerator of  $Z_{CSRf}(s)$  in Eq. (15) is smaller than that of  $Z_{CMVF}(s)$  in Eq. (14). In addition, the coefficients  $D'_1$  and  $D'_2$  in the denominator of  $Z_{CSRf}(s)$  are larger than  $D_1$  and  $D_2$  in  $Z_{CMVF}(s)$ , as shown in Eq. (16). Moreover, CSRf satisfies the passivity condition for the impedance function  $Z_{gen}(s) (= Z_{CSRf}(s)/s)$ . Under the control parameter conditions in Table 1,  $Z_{gen}(s)$  is asymptotically stable and  $Re(Z_{gen}(j\omega)) \geq 0$  [28]. The latter condition can be satisfied because there is no integrator in  $C_1(s)$ .

Additionally, an experiment to evaluate impedance performance under disturbance was conducted. For this purpose, the displacement  $x_l$  was disturbed using a position-controlled linear actuator at the end of a force-controlled SEA, instead of simulating human movements. The experimental setup is illustrated in Fig. 10a, and the experiment parameters are listed in Table 1.

Figure 10b displays the  $x_l$  plot created by the external actuator moving at the end of the SEA with a frequency of 1 Hz and an amplitude of 10 nm. The desired force was set at 100 N, with  $x_l$  applied after 3 s. Figure 10c shows the output force of the SEA at that time. Both controllers exhibit no significant error until 3 s. However, the error with CMVF then increases to 44.37 N, whereas CSRf exhibits a maximum error of only 2.86 N.

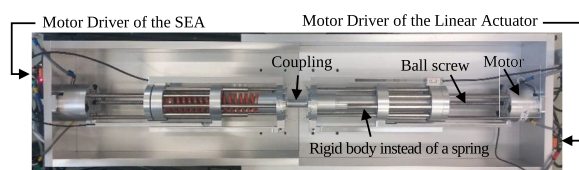
### 3.2 Functional sequence of exercise using the device

The Big 3 exercises using the device proceed in the following order when using the device (a reference video clip is available in [29]). Initially, the supporting boards of the two modules are fixed when the subject rides on the device and takes a posture according to the protocol. During this phase, the gravitational force  $F_g$  is measured, with the subject instructed to relax their entire body.

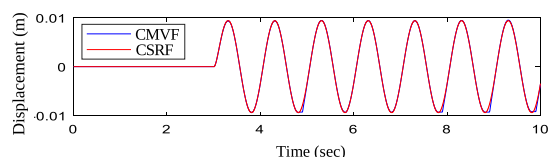
As the measurement commences,  $F_{assist}$  is linearly decreased from the maximum force. The supporting board falls when  $F_{assist}$  becomes lower than  $F_g$ . We determine that  $F_g$  equals  $F_{assist}$  when  $F_g$  drops below a specific threshold

**Table 1** SEA Parameters in the system

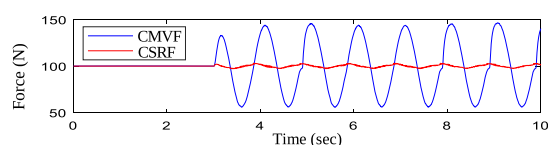
Subsystem	Parameters	Values
Plant	Dynamic mass, $m$ (kg)	453
	Damping ratio, $b$ (N·s/m)	3196
	Spring stiffness, $k_s$ (kN/m)	15.7
Controller	P gain of $C_1(s)$ , $K_{p,f}$ ( $m \cdot s^{-1} \cdot N^{-1}$ )	1.2998e-03
	D gain of $C_1(s)$ , $K_{d,f}$ ( $m \cdot s^{-2} \cdot N^{-1}$ )	4.2296e-05
	P gain of $C_2(s)$ , $K_{p,v}$ (N·s/m)	4.0058e+04
	I gain of $C_2(s)$ , $K_{i,v}$ ( $N \cdot s^2/m$ )	2.8752e+05



(a) Test bed for free end of the SEA with a linear actuator for disturbance motion



(b) Displacement of disturbance motion by the linear actuator



(c) Output Force of the SEA

**Fig. 10** Experiment of a position-controlled actuator applying disturbance at the end of SEA

position of the SEA (3 mm from the initial position). The measured  $F_g$  represents the gravitational force at the SEA's assist force point. This method allows for the estimation of the segmental masses of the upper body  $F_{g,u}$  and lower body  $F_{g,l}$ , as shown in Fig. 8b, d, and g.

At the exercise's outset, the device applies a constant force  $F_{assist}$  using the SEA, based on the given assistance ratio  $\alpha$ . Since  $F_g$  exceeds  $F_{assist}$ , the supporting board is no longer fixed, requiring the patient to maintain the exercise posture. At the exercise's conclusion, the supporting boards are re-fixed, completing one exercise cycle.

### 3.3 Subjects and experiment procedure

We selected 20 healthy men without LBP or other diseases for the evaluation experiment, using the Oswestry Disability Index (ODI) as the screening tool. The ODI is the most commonly used questionnaire for measuring the percentage score of LBP severity. The details of the subjects are provided in Table 2.

The subjects performed each of the Big 3 exercises in both calisthenics and using the proposed device. The assistance ratio  $\alpha$  was set to 75, 80, 85, 90, and 95% for the Big 3 exercises when performed with the proposed device. In determining the assistance ratios for the device, the values were set arbitrarily during its development phase. It was noted that when participants exercised using the device, performing the exercises became challenging at assistance levels

below 75%. Therefore, we established 75% as the minimum assistance level and divided the assistance ratios into five distinct levels, with each level differing by 5 percentage points. Additionally, these  $\alpha$  values were chosen to be relatively high in order to observe significant load changes even with minor adjustments in load. Therefore, exercising with the device at high  $\alpha$  settings is expected to reduce the lumbar load compared to performing calisthenics. Simultaneously, lumbar muscle activities were measured using sEMG sensors during the exercises.

A questionnaire survey was also conducted to investigate the differences in load on the lumbar and other body parts when performing calisthenics compared to exercises using the device. All experimental procedures were approved by the Seoul National University Institutional Review Board (IRB No. 1709/003-005), and all research was conducted in accordance with relevant regulations. Additionally, informed consent was obtained from all participants. Finally, the three individuals appearing in the images of the experimental procedure, as shown in Fig. 11, are members of the research team. They have provided consent for the publication of their identifying information and images in this paper.

### 3.4 Surface electromyography and signal processing

We utilized the DELSYS Trigno Wireless EMG system to measure muscle activity. Five sEMG sensors were attached to the RA, EO, IO, TE, and LE muscles. The attachment loca-

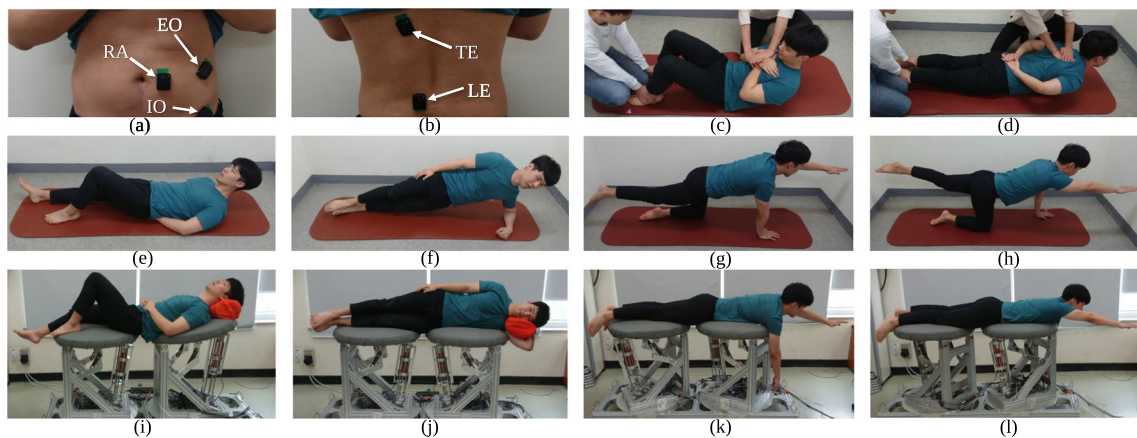


**Fig. 11** Experimental posture and sequence: **a** sEMG sensors locations of RA, EO, and IO, **b** sEMG sensors locations of TE and LE, **c** MVIC measurement of RA, EO, and IO, **d** MVIC measurement of TE and LE, **e** curl-up, **f** side-bridge, **g** bird-dog lifting a left hand and a right leg, **h**

bird-dog lifting a right hand and a left leg, **i** curl-up (using the device), **j** side-bridge (using the device), **k** bird-dog lifting a left hand and a right leg (using the device), and **l** bird-dog lifting a right hand and a left leg (using the device)

tions for the sensors are specifically positioned as follows: on the RA, 3 cm lateral to the umbilicus; on the EO, approximately 15 cm lateral to the umbilicus and aligned transversely with it; on the IO, positioned below the EO electrodes and just superior to the inguinal ligament; on the TE, 5 cm lateral to the T9 spinous process; and on the LE, 3 cm lateral to the L3 spinous process. These placements are depicted in Fig. 11a, b.

The measurements at IO and LE also reflect the activity of the transverse abdominis and quadratus lumborum, respectively [30]. Raw data from the sEMG sensors were sampled at a frequency of 2 kHz and processed through a sixth-order Butterworth band-pass filter with a frequency range of 10–500 Hz. A root mean square filter with a window size of 200 samples was subsequently used for signal smoothing.

For the evaluation of normalized sEMG data, the maximum voluntary isometric contraction (MVIC) method was conducted before performing the two types of exercises [14]. The first involves a flexion measurement to normalize the RA, EO, and IO muscles. The subject lies down straight and performs a flexion motion, lifting the upper body with maximum force, as shown in Fig. 11c. The second involves an extension

measurement to normalize the TE and LE muscles. The subject lies prone and performs an extension motion, lifting the upper body with maximum force, as illustrated in Fig. 11d. Finally, the final value of muscle activity is obtained using the acquired normalized MVIC values.

## 4 Experiment results

### 4.1 Experimental sequence

After the MVIC measurements, four groups of isometric exercises were performed: CU, SB, bird-dog lifting the left hand and right leg (BDL), and bird-dog lifting the right hand and left leg (BDR). Each exercise was performed for 15 s and repeated three times. To avoid muscle fatigue, there was a 30-second break between repetitions of the same exercise and a 60-second break between different exercises.

The exercise sequence for each group was as follows: First, the subjects performed calisthenics for the Big 3 exercises, as depicted in Fig. 11e–h. Then, the subjects took the postures according to the exercise protocol using the device, as shown in Fig. 11(i)–(l). During these two stages, only instructions related to maintaining the correct posture were given. The assistance ratio  $\alpha$  was adjusted from 95% to 75% in decrements of 5% for each set of exercises. After each exercise, the subjects completed a questionnaire survey regarding the perceived load on the lumbar region and other body parts.

### 4.2 Method of statistical analysis

The statistical analyses aimed to evaluate whether the exercises performed using the device meet the intended goals.

**Table 2** Subject characteristics (Male,  $n = 20$ )

Variable	Mean	±	SD
Age (years)	22.95	±	1.93
Height (cm)	176.28	±	4.33
Weight (kg)	74.37	±	7.04
BMI ( $kg/m^2$ )	23.91	±	1.83
ODI (%)	2.67	±	3.02

SD standard deviation, BMI body mass index, ODI Oswestry Disability Index

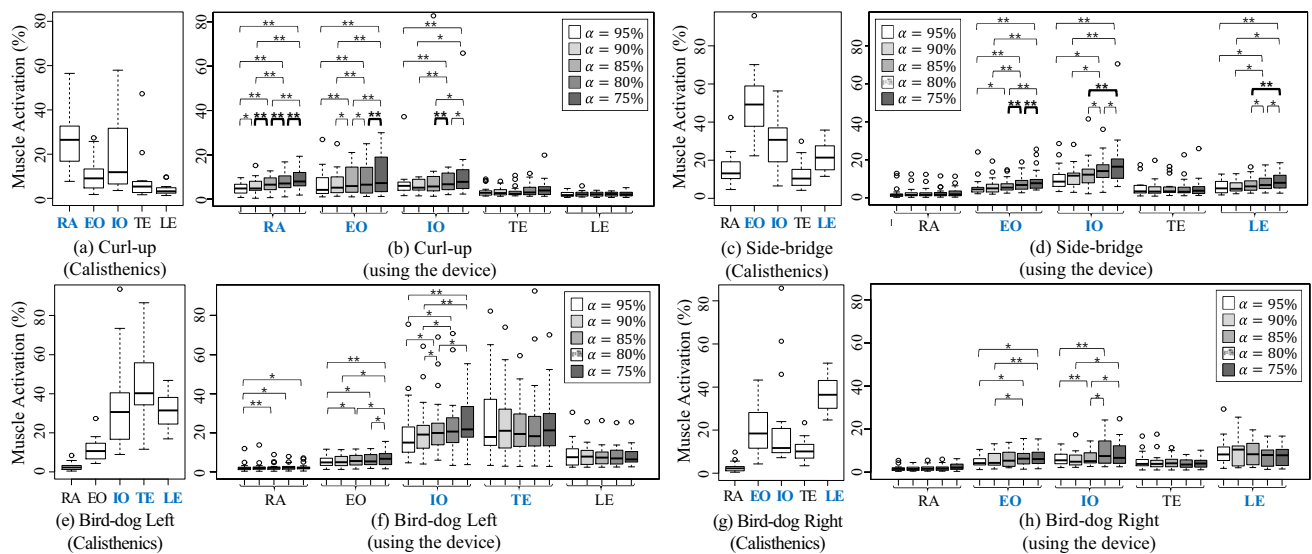


**Fig. 12** Box plots of muscle activity calculated from sEMG measurement of the calisthenics and the exercises using the device. (CU: curl-up, SB: side-bridge, BDL: bird-dog lifting a left hand and right leg, BDR: bird-dog lifting a right hand and left leg)

For an intuitive comparison of the sEMG data, the box plots of the muscle activities calculated from the experiments are presented in Fig. 12. Exercise sessions using the device showed overall lower muscle activities compared to calisthenics, attributable to the high assist ratio  $\alpha$ , as outlined in the experimental procedure. Moreover, since the muscle activities of each muscle in the 20 patients did not satisfy normality, nonparametric methods were utilized in the statistical analysis. All statistical analyses were conducted using IBM SPSS version 23.0.

**Analysis 1. Training Muscles:** To validate the design goal, we classified the training muscles in both calisthenics and the exercise using the device, confirming that they exhibited similar tendencies. In the exercises performed with the device, those with  $\alpha = 75\%$  which have the lowest device assistance and the highest exercise loads were selected for statistical analysis. Based on the median muscle activity, the top three muscles with the highest activity were identified as the training muscles among the five measured muscles. These significantly more active upper three muscles were then compared to the less active lower two muscles using the Mann–Whitney test, with a significance level set at  $p < 0.05$ . The classified muscles are highlighted in bold blue letters on the horizontal axis in Fig. 12.

**Analysis 2. Adjustment of the Load:** We analyzed the differences in lumbar muscle activities across five different  $\alpha$  values to assess the impact of load adjustment on the device’s performance. The Friedman test, a nonparametric alternative to the one-way repeated measures ANOVA, was conducted. If significant differences ( $p < 0.05$ ) were identified in the Friedman test, the Wilcoxon signed-rank test was used as a *post hoc* analysis. In this analysis, the Bonferroni

correction ( $p < 0.01 = 0.05/5$ ) for the five  $\alpha$  values was applied when determining significance. Cases where exercises with a lower  $\alpha$  exhibited higher muscle activity are indicated in Fig. 12 with \* and \*\*, for conditions  $p < 0.05$  and  $p < 0.01$ , respectively.

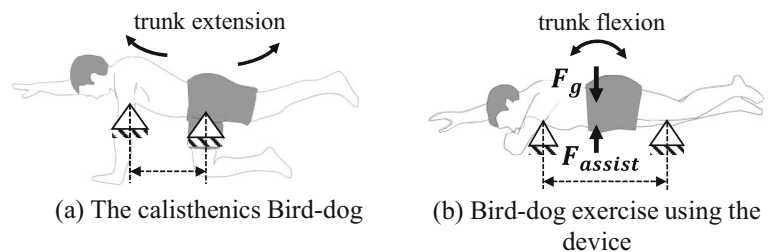
### 4.3 Results of statistical analysis

**Curl-up (CU):** In *Analysis 1*, the muscles (RA, EO, and IO, indicated in bold blue letters in Fig. 12a, b) were identified as the primary training muscles for the CU exercise, both in calisthenics and when using the device, thus fulfilling the design goal. As anticipated, the proportion of RA activity among the training muscles decreases when using the proposed device compared to calisthenics. The results of *Analysis 2* are also illustrated in Fig. 12b. Increased muscle activity with statistically significant differences (\* and \*\*) is predominantly observed when  $\alpha$  is reduced. Specifically, the results for RA align most closely with the desired outcome. In all cases except one (the difference between  $\alpha$  of 95% and 90%), differences with a Bonferroni corrected significance level (\*\*) are noted.

Among the cases with significant differences ( $p < 0.01$ ), those with the smallest load difference (indicated by bold \*\* in Fig. 12b) are as follows: For RA, a significant difference in muscle activity of 1.74%, 0.54%, and 0.89% is observed between  $\alpha$  levels of 90% and 85%, 85% and 80%, and 80% and 75%, respectively. EO exhibits a difference in muscle activity of 0.73% for a significant difference between  $\alpha$  of 80% and 75%, while IO shows a difference in muscle activity of 1.02% for a significant difference between  $\alpha$  of 85% and 80%. These values are smaller compared to those observed



**Fig. 13** Static analysis of the experiment results of bird-dog exercise



with conventional exercise methods (5–15%). The results validate that the proposed device facilitates improved fine load adjustment during exercise.

**Side-bridge (SB):** The results of the side-bridge exercises, as shown in Fig. 12c and d, align with the set objectives. In *Analysis 1*, the EO, IO, and LE muscles were identified as training muscles for both the calisthenics and the exercises using the device. In *Analysis 2*, significant differences in muscle activity were observed in most cases when varying  $\alpha$  during the SB exercises using the device. The number of cases showing significant differences is slightly fewer than in the CU exercises.

When using the proposed device for SB exercises, the significant differences in muscle activity (indicated by bold \*\* in Fig. 12d and  $p < 0.01$ ) are also smaller than those observed with conventional methods (5–15%). For EO, significant differences in muscle activity are noted between  $\alpha$  levels of 85% and 80%, and between 80% and 75%, measured at 1.53% and 0.90%, respectively. Results for the IO and LE muscles also exhibit significant differences in muscle activity of 4.29% and 1.58%, respectively, between  $\alpha$  levels of 85% and 75%.

**Bird-dog (BD):** In the BD experiment, two variations were performed: bird-dog lifting left hand and right leg (BDL) and bird-dog lifting right hand and left leg (BDR). The rationale for conducting these two exercises was to measure the muscle activity of the 10 lumbar muscles on both the left and right sides due to the diagonal axis of rotation passing through the body. The results for BDL are presented in Fig. 12e and f, while those for BDR are shown in Figs. 12g and h.

In *Analysis 1*, the IO, TE, and LE muscles were identified as training muscles in the calisthenics BDL. However, LE was not classified as a training muscle in the exercise using the device. This change is attributed to the fact that in the proposed device, the left leg, which is typically used for posture maintenance in calisthenics, remains almost fixed, resulting in less activation of the LE muscle. In the BDR variation, the training muscles when using the device align with those in calisthenics, thereby fulfilling the design goal of training the same muscles as expected.

During *Analysis 2*, unlike the results for CU and SB, unexpected outcomes were observed. Among the IO and TE

muscles, which were classified as training muscles in the BDL, only the load on IO was adjusted with changes in  $\alpha$ . Additionally, the load on the EO muscle, which was not classified as a training muscle, was also adjusted in response to changes in  $\alpha$ .

In the BDR exercises, the load on the LE muscle, one of the training muscles, did not adjust as expected for the following reasons: In BD calisthenics, trunk extension is achieved by lifting the arms and legs, as illustrated in Fig. 13a. However, when exercising with the device, a torque related to trunk flexion is required to counteract abdominal drooping due to gravitational force  $F_g$ ; therefore, the SEA is positioned in the abdomen area, as described in Fig. 8g. The experimental results indicate adjustments in RA, EO, and IO activities, suggesting that the SEA contributes to trunk flexion, as shown in Fig. 13b.

The median values of the TE muscles during BDL in Fig. 12f and the LE in BDR in Fig. 12h demonstrate a reduced load with decreasing  $\alpha$ , contrary to the load adjustments observed in the training muscles for CU and SB. This discrepancy is likely due to the decreasing trunk extension torque as the trunk flexion torque increases.

#### 4.4 Result of questionnaire survey

After completing the experiment, the participants were asked to fill out a survey questionnaire to verify the study's objectives. The survey focused on investigating the differences in perceived load on body parts other than the lumbar region when performing calisthenics compared to exercising using the device. The questions and results of the survey are presented in Table 3, with further details of the questionnaire described in [16].

Most participants reported feeling a load on other body parts during the three calisthenics exercises. Specifically, the neck was predominantly affected during CU, and the shoulder during SB and BD. In contrast, most participants noted a decrease in the load on other body parts when exercising with the proposed device, especially noticeable in the SB exercises.



**Table 3** Results of the questionnaire survey

	Questions	Answers	CU	SB	BD
After	Feel the load on parts other than lumbar	Yes	16	20	16
Calisthenics	Which body part	Most voted	neck	shoulder	Shoulder
After using	How has load of parts	Increase	6	4	6
The device	Other than lumbar changed	Decrease	12	18	10

## 5 Discussion

The results suggest that the proposed method can control the load more precisely than conventional methods. Notably, the results of the CU and SB exercises show significant differences in muscle activity of less than 5% when altering the assistance ratio  $\alpha$  for the training muscles. Consequently, when designing an appropriate protocol using the proposed system, the muscle load for the desired LSE can be precisely adjusted. This precision allows for the provision of adequate, pain-free exercise loads to patients, thereby facilitating the restoration of spinal stability through progressive and incremental fine loads.

In conclusion, while this study demonstrates the potential of the proposed device in optimizing lumbar stabilization exercises, there are several avenues for future exploration and improvement.

First of all, the BD exercise provides a direction for future research. In BD, the training muscles predominantly used when exercising with the device were the same as those in calisthenics. However, the expected load adjustment on these training muscles was not observed. Unlike simpler exercises like CU and SB, which apply torque in a single direction, more complex movements like BD require an improved design method. Therefore, future research should focus on enhanced design methodologies, such as those based on human body modeling, when developing exercise protocols using the proposed device.

The questionnaire survey also has limitations. As mentioned in the questionnaire survey section, exercising using the device results in an overall lower load compared to calisthenics. For more accurate survey results regarding the loads on body parts other than the lumbar region, load conditions similar to those in calisthenics should be considered. Therefore, additional experiments with increased loads are required. In addition to survey methods, it would also be beneficial to attach sEMG sensors to other parts of the body to measure muscle activity and thereby assess changes in the load on the other body parts.

Moreover, the integration of advanced biomechanical modeling and simulation techniques could enhance the device's adaptability and precision, tailoring it to individual user needs. This personalization aspect is particularly

important in therapeutic settings, where exercises must be customized to address specific patient conditions. It is necessary to predict loads on parts other than the lumbar region using model-based dynamic simulations and to verify these predictions through various sEMG experiments. Additionally, through modeling methods, it would be possible to develop exercise protocols optimized for exercises using the device.

Lastly, for safety reasons, the experiment was conducted with healthy subjects in this study. Future research will involve conducting additional experiments with actual low back pain patients to verify the effectiveness of exercising using the device. Additionally, exploring the device's long-term impact on various user groups, especially those with chronic low back pain, will be crucial in understanding its clinical efficacy and safety.

## 6 Conclusion

This study proposes a novel device designed to quantitatively and precisely adjust the lumbar load while simultaneously reducing the load on other body parts in lumbar stabilization exercises. The device accurately regulates the lumbar load using series elastic actuators without the need for changing the exercise posture. Moreover, it enables the gradual reduction of muscle load by progressively increasing the assistive force applied to the target lumbar muscles.

An experimental evaluation involving 20 healthy male subjects performing three types of exercises verified the improved performance of the proposed method. In particular, the surface electromyography measurements for the curl-up and side-bridge exercises, which require unidirectional lumbar torque, demonstrated that the same muscles trained by calisthenics were engaged. Furthermore, the load on these muscles could be adjusted using the device. Notably, when adjusting the load, there was a statistically significant difference in muscle activities (<5%) compared to conventional calisthenics methods. However, for the bird-dog exercises, which require more complex torque than CU and SB, the device engaged the target muscles as expected, but some muscle loads were not adjusted as intended. This outcome suggests the need for future improvements in the design of exercise protocols. Lastly, the questionnaire survey revealed

that the load on body parts other than the lumbar region decreased in all three exercises when using the device.

**Acknowledgements** This work was supported by the National Research Foundation of Korea (NRF) grant funded by the Korea government (MSIP) (No. NRF-2015R1A2A1A10055798).

**Funding** Open Access funding enabled and organized by Seoul National University.

## Declarations

**Conflict of interest** The authors declare no conflict of interest.

**Open Access** This article is licensed under a Creative Commons Attribution 4.0 International License, which permits use, sharing, adaptation, distribution and reproduction in any medium or format, as long as you give appropriate credit to the original author(s) and the source, provide a link to the Creative Commons licence, and indicate if changes were made. The images or other third party material in this article are included in the article's Creative Commons licence, unless indicated otherwise in a credit line to the material. If material is not included in the article's Creative Commons licence and your intended use is not permitted by statutory regulation or exceeds the permitted use, you will need to obtain permission directly from the copyright holder. To view a copy of this licence, visit <http://creativecommons.org/licenses/by/4.0/>.

## References

- Duthey B (2013) Background paper 6.24 low back pain. Priority medicines for Europe and the world. *Glob Burden Dis* 2010:1–29
- Hoy D, Bain C, Williams G, March L, Brooks P, Blyth F, Woolf A, Vos T, Buchbinder R (2012) A systematic review of the global prevalence of low back pain. *Arthritis Rheumatol* 64(6):2028–2037
- Andersson GB (1999) Epidemiological features of chronic low-back pain. *The lancet* 354(9178):581–585
- Gore M, Sadosky A, Stacey BR, Tai K-S, Leslie D (2012) The burden of chronic low back pain: clinical comorbidities, treatment patterns, and health care costs in usual care settings. *Spine* 37(11):668–677
- Chou R, Qaseem A, Snow V, Casey D, Cross JT, Shekelle P, Owens DK (2007) Diagnosis and treatment of low back pain: a joint clinical practice guideline from the American college of physicians and the American pain society. *Ann Intern Med* 147(7):478–491
- Hildebrandt J, Ursin H, Mannion AF, Airaksinen O, Brox JI, CEDRASCHI C, Kovacs F, Reis S, Staal B, Zanoli G, et al (2004) European guidelines for the management of chronic non-specific low back pain. Norway: European Commission, Research Directorate-General, Department of Policy, Co-ordination and Strategy
- Koes BW, van Tulder M, Lin C-WC, Macedo LG, McAuley J, Maher C (2010) An updated overview of clinical guidelines for the management of non-specific low back pain in primary care. *Eur Spine J* 19(12):2075–2094
- Panjabi MM et al (1992) The stabilizing system of the spine. part ii. neutral zone and instability hypothesis. *J Spinal Disord* 5:390–390
- Richardson C (2004) Therapeutic exercise for lumbopelvic stabilization: a motor control approach for the treatment and prevention of low back pain. Churchill Livingstone, London
- McGill SM (2015) Low back disorders, 3E. Human Kinetics, Champaign
- Wang X-Q, Zheng J-J, Yu Z-W, Bi X, Lou S-J, Liu J, Cai B, Hua Y-H, Wu M, Wei M-L et al (2012) A meta-analysis of core stability exercise versus general exercise for chronic low back pain. *PLoS ONE* 7(12):52082
- Hides JA, Jull GA, Richardson CA (2001) Long-term effects of specific stabilizing exercises for first-episode low back pain. *Spine* 26(11):243–248
- Standaert CJ, Weinstein SM, Rumpeltes J (2008) Evidence-informed management of chronic low back pain with lumbar stabilization exercises. *Spine J* 8(1):114–120
- Choi W, Won J, Cho H, Park J (2017) A rehabilitation exercise robot for treating low back pain. In: 2017 IEEE international conference on robotics and automation (ICRA), pp 482–489. IEEE
- Kim J, Choi W, Hur S, Park J (2021) Advanced compliant anti-gravity robot system for lumbar stabilization exercise using series elastic actuator. *IEEE J Trans Eng Health Med* 10:1–11
- Cho H, Choi W, Kim J, Park J (2018) Performance evaluation of lumbar stabilization exercise robot considering body load. In: The 13th Korea robotics society annual conference, 2018. KRoC 2018. KROS
- O'Sullivan PB (2000) Masterclass. lumbar segmental 'instability': clinical presentation and specific stabilizing exercise management. *Man Ther* 5(1):2–12
- Kofotolis N, Kellis E (2006) Effects of two 4-week proprioceptive neuromuscular facilitation programs on muscle endurance, flexibility, and functional performance in women with chronic low back pain. *Phys Ther* 86(7):1001–1012
- Panjabi MM (2003) Clinical spinal instability and low back pain. *J Electromyogr Kinesiol* 13(4):371–379
- Yoon T-L, Cynn H-S, Choi S-A, Choi W-J, Jeong H-J, Lee J-H, Choi B-S (2015) Trunk muscle activation during different quadruped stabilization exercises in individuals with chronic low back pain. *Physiother Res Int* 20(2):126–132
- Souza GM, Baker LL, Powers CM (2001) Electromyographic activity of selected trunk muscles during dynamic spine stabilization exercises. *Arch Phys Med Rehabil* 82(11):1551–1557
- Lehman GJ, Hoda W, Oliver S (2005) Trunk muscle activity during bridging exercises on and off a swissball. *Chiropr Osteopat* 13(1):14
- Centaur. Accessed 31 Aug 2018. <http://www.bfmc.info/eng/index.php?cs=4-1>
- McGill SM, Karpowicz A (2009) Exercises for spine stabilization: motion/motor patterns, stability progressions, and clinical technique. *Arch Phys Med Rehabil* 90(1):118–126
- McGill S (2015) Low Back Disorders: Evidence-based Prevention and Rehabilitation. Human Kinetics
- McGill SM (1998) Low back exercises: evidence for improving exercise regimens. *Phys Ther* 78(7):754–765
- Vallery H, Ekkelenkamp R, Van Der Kooij H, Buss M (2007) Passive and accurate torque control of series elastic actuators. In: 2007 IEEE/RSJ international conference on intelligent robots and systems, pp 3534–3538. IEEE
- Colgate JE (1988) The control of dynamically interacting systems. PhD thesis, Massachusetts Institute of Technology
- Sequential progression of the exercise using the SERA system. Accessed 31 Oct 2022. <https://youtu.be/xFJLHEfow4Q>
- McGill S, Jucker D, Kropf P (1996) Appropriately placed surface emg electrodes reflect deep muscle activity (psoas, quadratus lumborum, abdominal wall) in the lumbar spine. *J Biomech* 29(11):1503–1507

**Publisher's Note** Springer Nature remains neutral with regard to jurisdictional claims in published maps and institutional affiliations.